Computer tomography of infra-red absorption and its application to internal-combustion engines

By

H Kawazoe and J H Whitelaw

Mechanical Engineering Department
Imperial College of Science, Technology and Medicine
London SW7 2BX, UK

ABSTRACT

A comparatively inexpensive instrument has been developed for the measurement of local concentrations of gaseous fuel and evaluated in terms of its application to the flow in the cylinders of internal-combustion engines. It is based on the absorption of infra-red light by hydrocarbons and computer tomography to provide spatially local information. This paper describes the instrument and its application to the flow in simple arrangements intended to represent the cylinders of an internal-combustion engine with provision for optical access.

The optical system is comprised a helium-neon laser, a lead-selenium sensor, a chopper, an amplifier and a microcomputer. It can readily be modified to improve spatial resolution by monitoring the temporal fluctuations in the intensity of the laser beam, the error from which was reduced to less than 0.8% in the present experiment. A translation and rotation scanning method formed the basis for tomography and the spatial distribution of gaseous fuel was reconstructed by the convolution method with the filter function of Shepp and Rogan .

The instrument was applied to a simulation of the flow in a lean-burn gasoline engine, the cylinder of which was made of quartz glass for the measurement. The methane fuel was injected at the intake valve or 100 mm upstream of the valve to simulate evaporated fuel with steady airflow, and the port geometry provided swirl corresponding to the ratios of 1.3 and 2.9. The cylindrical cylinder surrounding the quartz glass implied that the fibre which detected the laser light absorption at local positions along the light path were located after calculation of the true position within the flow.

Distributions of the concentration of methane are presented in figure 1, corresponding to the higher ratio of swirling flow and plane 70 mm from the cylinder head with the fuel injected close to the valve. The laser beam was passed by the optical fiber at 5 mm spatial intervals and to angles, corresponding to 5 degrees for rotation in the plane. The measurement region encompassed the total area of each plane apart from that within 1.5 mm of the wall. The fuel-rich region with the swirl port spreads in the clockwise direction with the swirling flow.

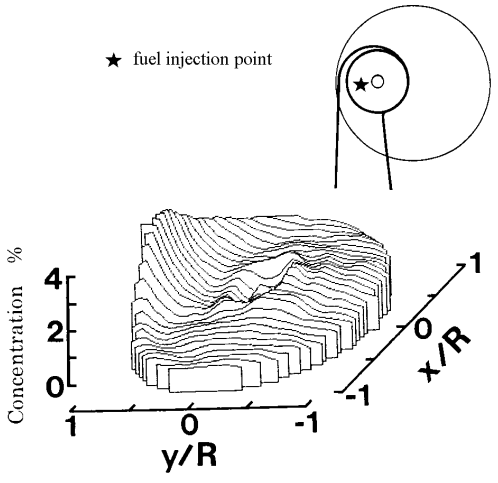

Fig.1 Fuel concentration of the swirl port with fuel injected at the intake valve (z=70mm).

1. INTRODUCTION

Recent development of an internal combustion engine, especially a lean burn gasoline engine of a direct fuel injection type has achieved such a drastic improvement in fuel consumption and exhaust emissions as over 20 %[1],[2]. For further development in a reciprocating engine as well as a gas turbine and a boiler, combustion phenomena in a combustion chamber should be analyzed in detail and more precise control of combustion will be required. Air-fuel mixture formation is a key factor from the point of view, and a new technology to investigate its process besides a laser Doppler anemometry (LDA), a phase Doppler analyzer (PDA) for a liquid fuel droplet and laser induced fluorescence (LIF) for gaseous fuel has been anticipated.

Although a lot of useful information and results has been reported by using LDA[3]-[5], PDA[6],[7] and LIF[8]-[10], reports concerned to gaseous fuel concentration in a combustion chamber, especially spatial and temporal distribution of gaseous fuel, are not been enough for a new engine to be developed and modified. Such a various kind of technologies as LIF, Rayleigh scattering[11], Mie scattering[12], two colour[13], infra-red ray absorption[14]-[18] and LIPF[19] methods for non-destructive measurement of gaseous fuel have been used. Each technology has advantages and disadvantages, and among them an LIF technology has been devised, placed on the market, and widely used to analyze combustion phenomena. However, a device system for an LIF measurement is huge, very expensive and too difficult to utilize easily for various combustion fields.

In this study, a compact and inexpensive instrument has been developed for the measurement of local concentrations of gaseous fuel and evaluated in terms of its application to the flow in the cylinders of internal-combustion engines. It is based on the absorption of infra-red light by hydrocarbons and computer tomography to provide spatially local information. This paper describes the instrument and its application to the flow in simple arrangements intended to represent the cylinders of an internal-combustion engine with provision for optical access.

2. COMPUTER TOMOGRAPHY BASED ON INFRA-RED LIGHT ABSORPTION

2.1 Infra-red Light Absorption

Infra-red light is absorbed by a fuel molecule based on vibration among atoms, that is modes of stretching and bending[20]. Hydrocarbon fuel has a strong infra-red light absorption by carbon-hydrogen bond's (C-H) stretching vibration, and figure 2 shows a light absorption spectrum of liquid paraffin. The light absorption of 2950cm^{-1} (wave length of about 3.4 μm) is caused by C-H stretch mode of vibration. This wave length fortunately coincides with 3.392μm line of a He-Ne laser.

Light absorption is influenced by a number of C-H bonds which is proportional to hydrocarbon fuel density, and it is presented by the following Lambert-Beer's law as shown in figure 3,

$$\frac{I}{I_0} = \exp[-\int_0^L f(x,y)dy] \qquad f(x,y) = a(x,y)\cdot c(x,y)$$

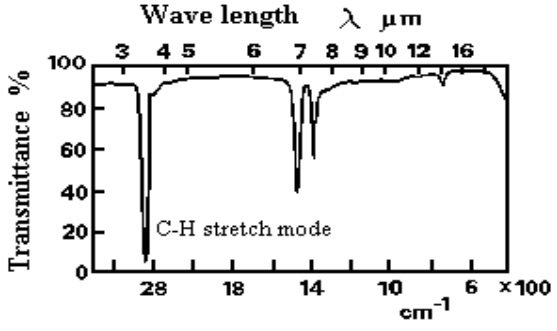

Fig.2 Spectrum of infra-red light

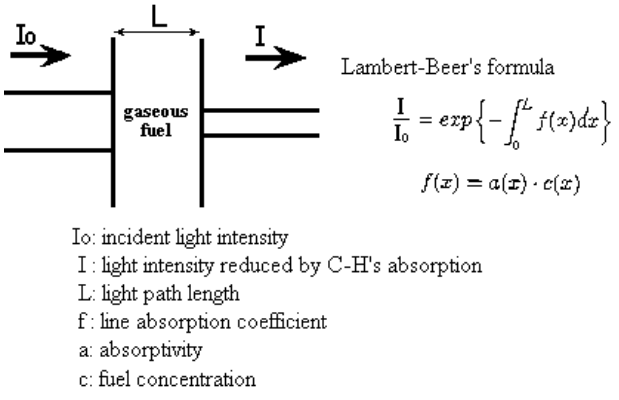

Fig.3 Infra-red light absorption by gaseous

absorbed by fluid paraffin. fuel according to Lambert-Beer's law.
where I_0 and I are incident light intensity and reduced one by fuel's absorption, and c and L are fuel concentration and length of incident light path, respectively. The constant of a, which is affected by fuel temperature and pressure[15] is a coefficient of absorption which is defined as absorptivity in this paper. The symbol of f for absorption per unit length of light path is called line absorption coefficient in the study.

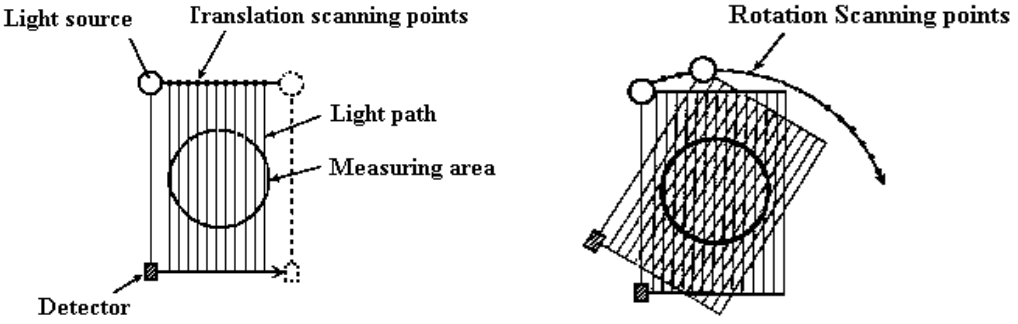

Fig.4 Translation-rotation (T-R) scanning for computer tomography.

2.2 Computer Tomograpy

Computer tomography is a well-known technology to investigate inner information of a human body in medical diagnostic field by using an X-ray. There are three types of typical measuring system which is according to scanning method of X-ray source and its corresponding detectors; translate-rotate (T-R), rotate-rotate (R-R), and stationary-rotate (S-R). Since the T-R method shown in figure 4 has such an advantage that it is faithful to the principal of computer tomography and has smaller effects by scattered light than the other methods, we have adopted the T-R method to measure fuel concentration in the study.

An inner cross-sectional information has been proved to be reconstructed by Radon[21] in 1917, and algorithm of reconstruction was reviewed by Gordon et al[22]. However, it could not be successful until computer technology has been developed due to necessity of enormous calculation for reconstruction of inner information. There are typical three methods for reconstruction; back projection, iterative approximation[23] and analytical methods. There are also three techniques in the analytical method; Fourier transformation[24], filtered back projection[25] and convolution[25],[26] techniques. We have adopted the convolution technique of the analytical method by the reason for shading of back projection technique as shown in figure 5 and empirical and tedious procedure of the iterative approximation method. The convolution technique revealed as the following equations has such an advantage that it does not need to be transformed into Fourier transformation field,

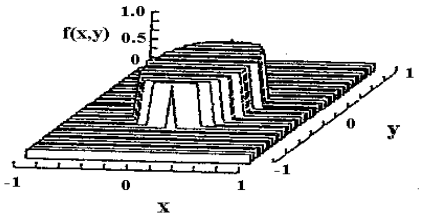

(a) Original image

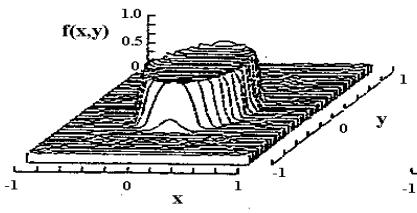

(b) Reconstructed by convolution methd

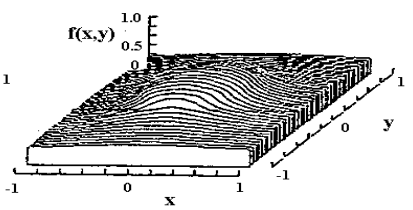

(c) Reconstructed by back projection

$$f(x,y) = \frac{1}{2p}\int_0^{2p} q(X,q)dq \qquad X = x\cos q + y\sin q$$

$$q(X,q) = \frac{1}{2}\int_{-\infty}^{\infty} g(t,q)\cdot h((X,t)dt \qquad h(X) = \frac{1}{2p}\int_{-\infty}^{\infty} H(w)e^{iwX}dw$$

Fig.5 Reconstruction of original image

where g, H and h are projection data, filter function and inverse Fourier transform of H, respectively. There are some kinds of filter function, and the function H(?) projected by Shepp and Rogan[26] was utilized in the research according to the report by Nakayama et al.[27] because of its small error and effective reconstruction for gaseous fuel without affection of high frequency such as by a droplet. The filter function of Shepp and Rogan is indicated in figure 6, and it has the slope of 1 at the origin and approaches to 0 at large value of independent variable ? , which gives higher accurate reconstruction.

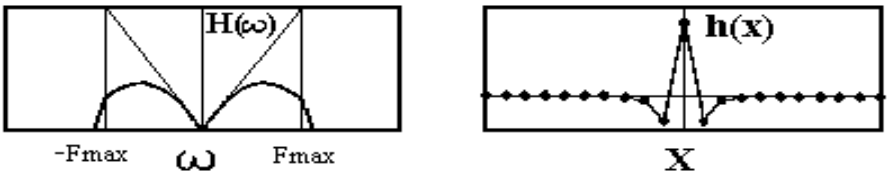

Fig.6 Shepp and Rogan's filter function[26].

3. EXPERIMENTAL DEVICES AND PROCEDURE

3.1 Measuring System

The optical system is shown in figure 7 and comprised a helium-neon laser (PMS Electro-Optics, LHIR-0100), a lead-selenium (PbSe) sensor (Hamamatsu Photonics, P2031-01), a chopper, an electrical amplifier and a microcomputer. Infra-red light of the He-Ne laser has the wave length of 3.392 μm and its maximum power is 2mW and it was shut on and off by the chopper for the PbSe sensors, the temperature of which was controlled to be constant by using the Peltier effect (Hamamatsu Photonics, C1103-02) for time-independent sensitivity of the sensor. Analog signal from the PbSe detector is amplified, changed to digital data, and stored in the microcomputer. Since the laser light is in the nature of fluctuation over 10%, it is divided to two beams by a quartz glass behind the chopper, and one of them is monitored to reduce this effect. It can improve spatial resolution by monitoring the temporal fluctuations in the intensity of the laser beam, the error from which was reduced to less than 0.8% in the present experiment as shown in figure 8.

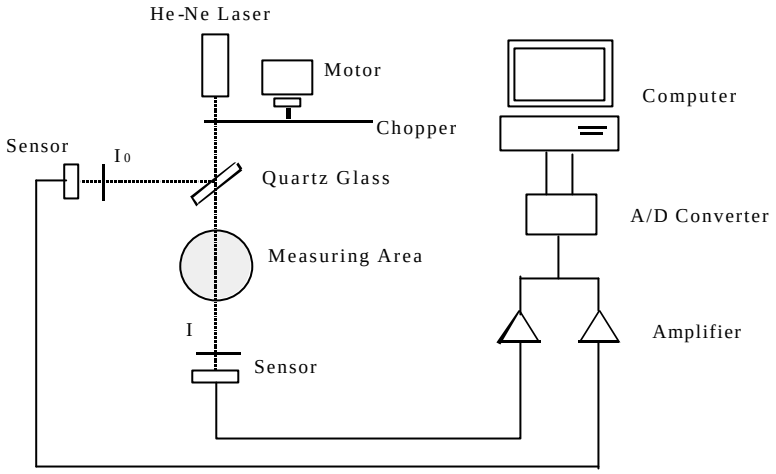

Fig.7 Optical system.

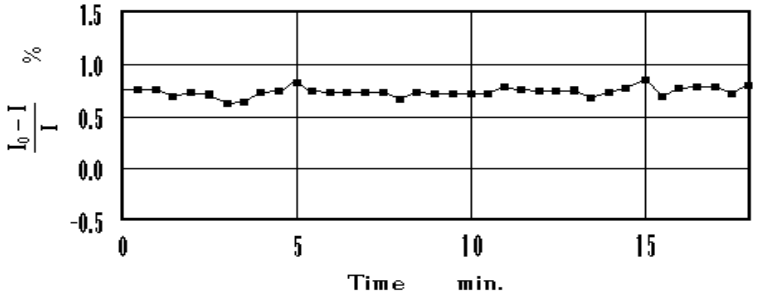

Fig.8 Effect of monitoring laser light intensity by the second PbSe sensor.

3.2 Engine Model

The instrument was applied to a simulation of the flow in the lean-burn gasoline engines shown in figure 9. The cylinder with the inner diameter of 83 mm was made of quartz glass, the methane fuel was injected at the intake valve or 100 mm upstream of the valve to simulate evaporated fuel with steady airflow, and the port geometry provided swirl corresponding to the ratios of 2.9 and 1.3. The former port with the swirl ratio of 2.9 is called swirl port and the latter is named straight port in the paper.

On the other hand, such a measurement as in-cylinder flow is one of the most difficult ones because existence of surrounding cylinder wall makes computer tomography measurement difficult. Therefore, The cylindrical cylinder surrounding the quartz glass implied that the fibre (Furukawa, Fluoride Fiber) which emitted the laser light and detected the reduced one by fuel's absorption at local positions along the light path were located after calculation of the true position within the flow, as shown in figure 10. The residual inner stress of the metal cylinder was removed by annealing twice in an autoclave prior to the manufacturing process for supporting the fibre at correct position. The manufacturing certainty of the aluminum-alloy cylinder is within 0.01mm for the location and 0.1 degree for the directions to hold the fibre probe.

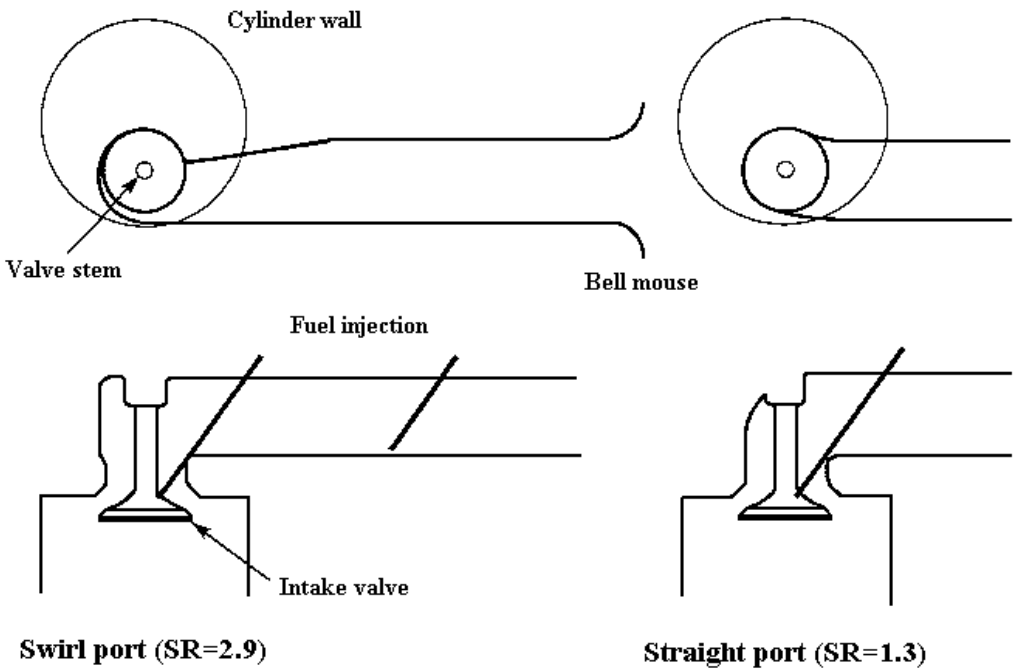

Fig.9 Modeled internal combustion gasoline engines.

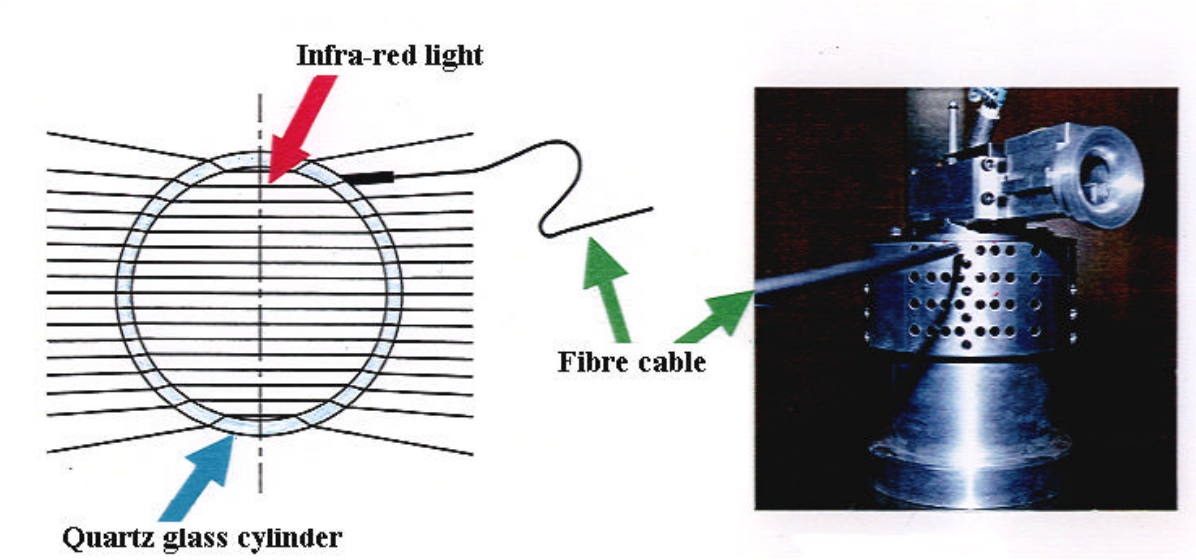

Fig.10 Predicted light path in the cylinder and its realization by an infra-red fibre.

3.3 Experimental Procedure

Verification by using a constant-volume cylindrical vessel with the same diameter of the model engine cylinder illustrated in figure 11 was carried out to determine fuel concentration, c, from reconstructed computer-tomography results, namely line absorption results, f(=a? c). The result of the calibration is shown in figure 12, where various symbols indicate the pressure of the initial and total air in the vessel with the pressure level

between 510 and 660 mmHg. The absorptivity, a, was calculated by the least square method based on the result, and fuel concentration was derived from reconstructed line absorption coefficients.

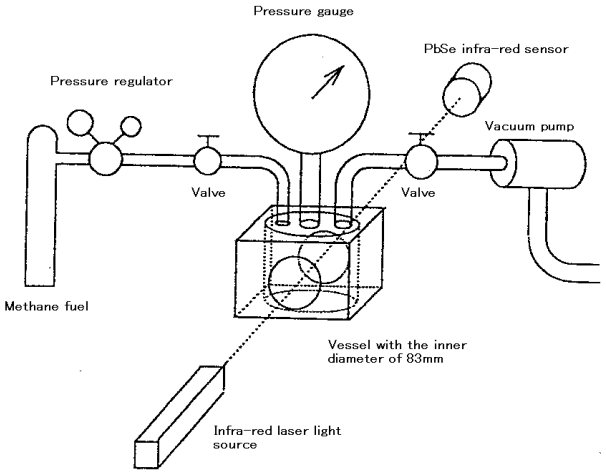

Fig.11 Experimental apparatus for verification of methane concentration.

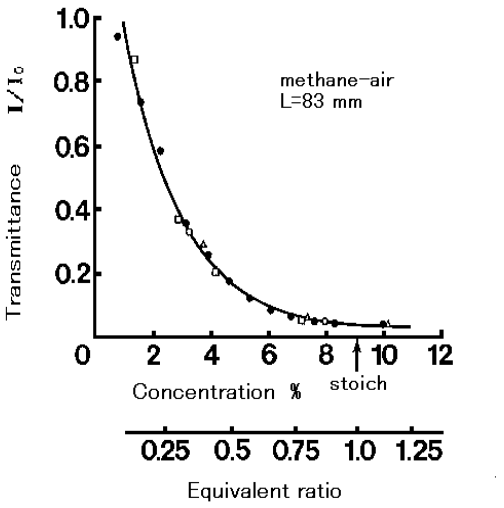

Fig.12 Verification results for methane fuel concentration.

Table 1 Experimental conditions

methane flow rate	110 cc/sec
airflow rate	6300 cc/sec
engine cylinder diameter	83 mm
intake valve lift	6 mm
intake port	? swirl port (swirl ratio SR=2.9) ? straight port (SR=1.3)
measured section	10 and 70 mm from cylinder head surface
computer tomography	? circle area : r=40 mm ? translate :? X=5mm ? rotate :? ? =5° ? sampling frequency : 20 kHz ? sampling time : 500 ms ? chopping frequency : 600 Hz ? infra-red He-Ne laser : 1 mW

Experimental condition is indicated in table 1, and distributions of the concentration of methane were measured for the two intake ports, corresponding to the two ratios of swirling flow and planes 10 and 70 mm from the cylinder head. The computer tomography measurements on the two cross sections were carried out separately, and the laser beam was passed by the optical fiber at 5 mm spatial intervals and to angles, corresponding to 5 degrees for rotation in each plane as shown in figure 10. Instead of rotation scanning, the part of the cylinder head was revolved around the centerline of the engine cylinder in the research. This translation and rotation scanning satisfied the favorable scanning relation indicated by the following equation,

$$N_{trans} \approx \frac{p}{2} \cdot N_{rot} + 1$$

where N_{trans} and N_{rot} are sampling numbers of translation and rotation, that is ray and view numbers. If the number of view is less than N_{rot} for a given N_{trans}, error of reconstruction would be enhanced, especially in the large gradient region of fuel concentration and it would produce such an artifact as a false line in the tangential direction. The measurement region encompassed the total area of each plane apart from that within 1.5 mm of the cylinder wall.

The chopping frequency of 600Hz gives the highest sensitivity of the infra-red sensor. Duration and frequency of sampling data are 500ms and 20kHz, respectively. Fuel concentration in the circle region with the radius of 40mm was investigated at the cross sections below 10 and 70mm from the cylinder head surface. Therefore, fuel in the region of 1.5mm outer of the measured circle was neglected in the measurement.

4. RESULTS

Gaseous fuel in the cylinder of a lean burn gasoline engine of an intake port fuel-injected type, which simulates the behavior of gasoline injected from a fuel injector to the intake valve, attached on valve tulip and evaporated here, was measured, and the results for the swirl port case are shown in figures 13 and 14 corresponding to the in-cylinder cross sections of 10 and 70 mm from the cylinder head. At upper cross section of the cylinder (z=10 mm), where z is distance from the surface of the engine cylinder head, most fuel appeared on the side of the cylinder wall just below the intake valve. The peak of the fuel concentration is 9.5% here against 1.7% of the homogeneous distribution, and it should be predicted that much richer concentration of fuel might be exist outer of the area. Apart from the region, fuel concentration drastically decreases and becomes flattened distribution.

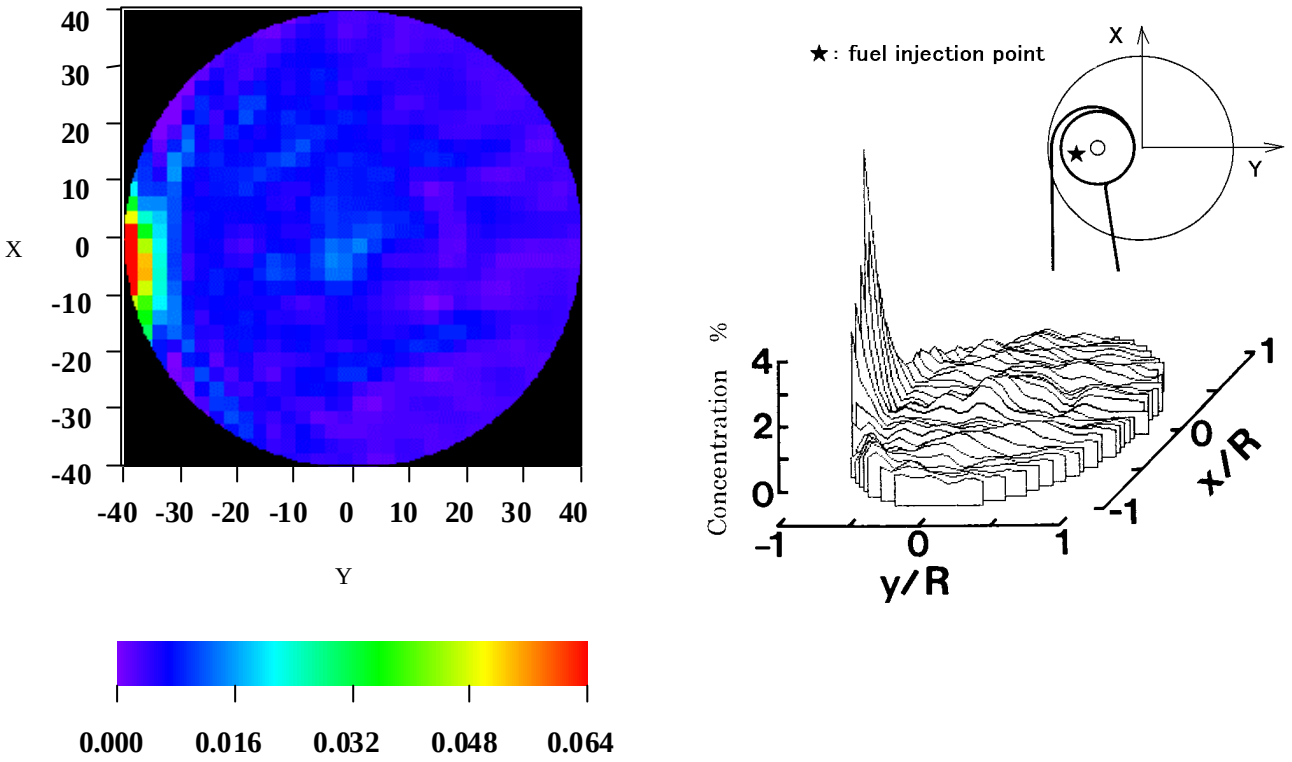

Fig.13 Methane concentration at the upper plane in the engine cylinder with the swirl port.

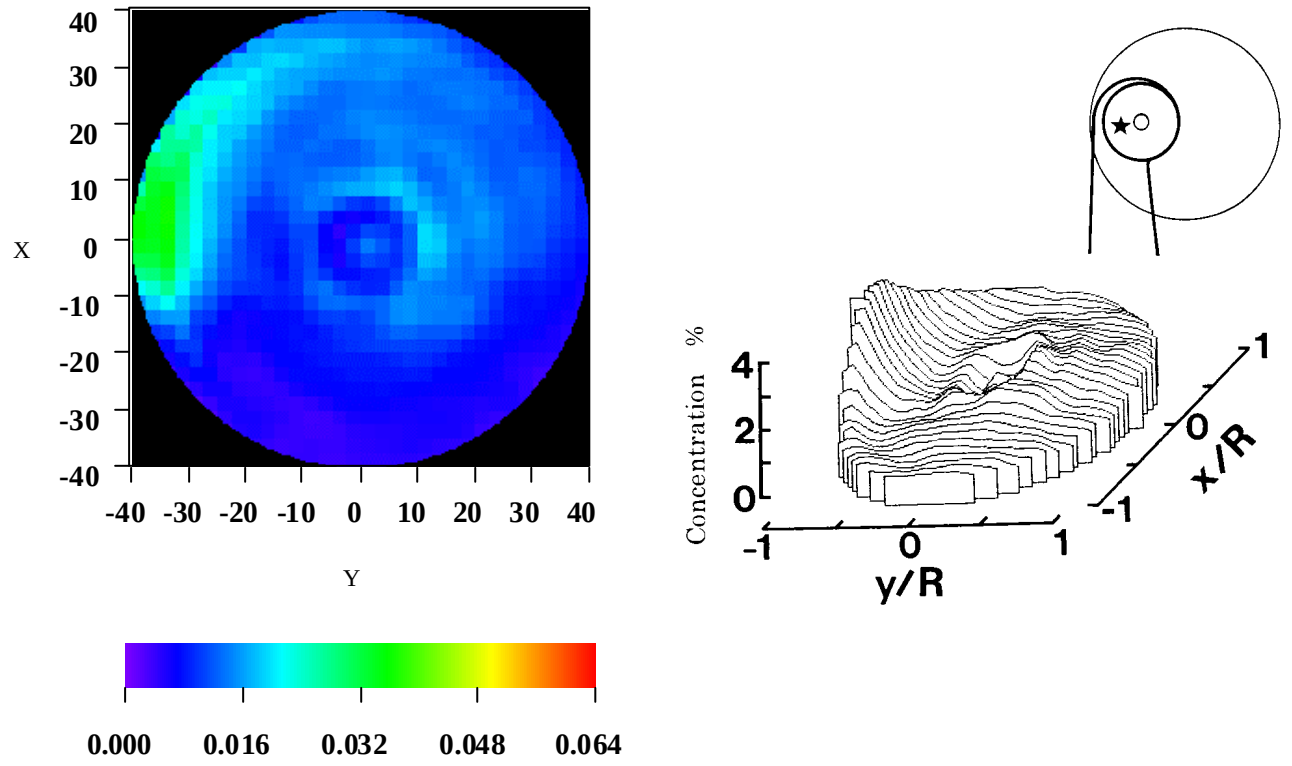

Fig.14 Methane concentration at the lower plane in the engine cylinder with the swirl port.

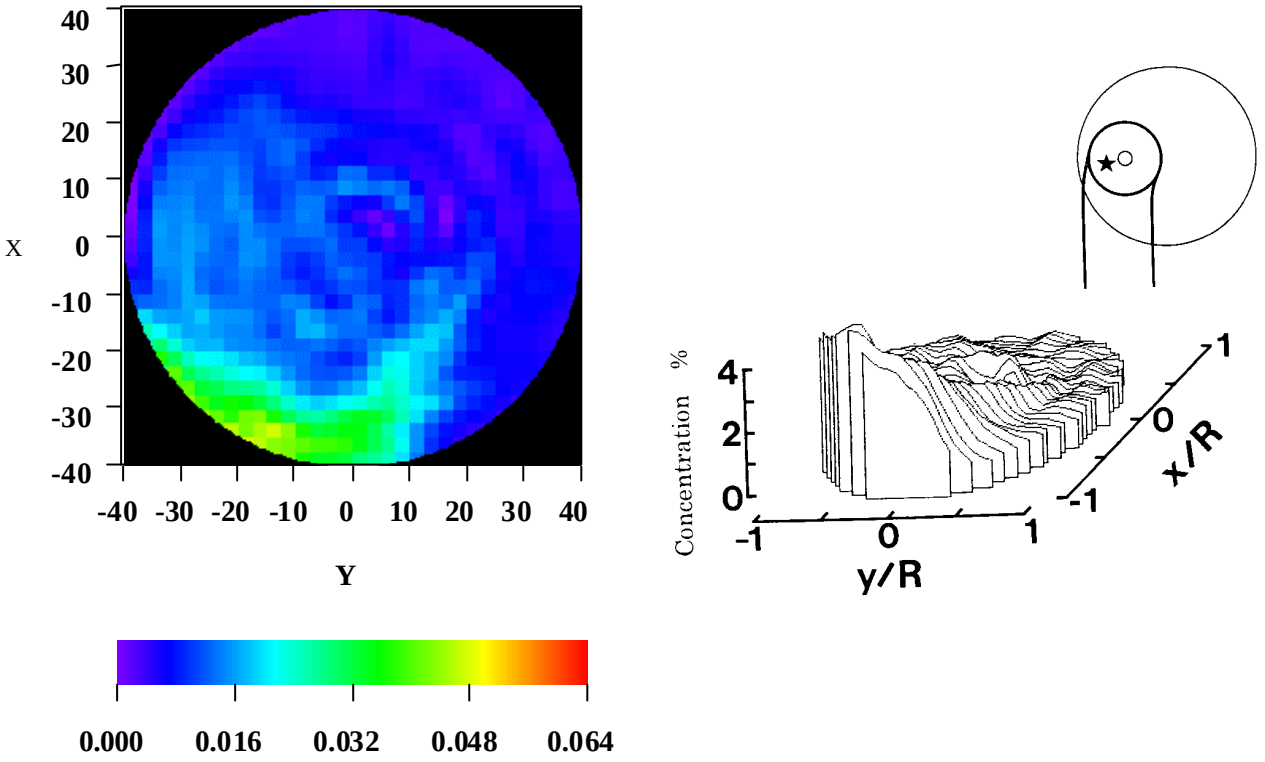

Fig.15 Methane concentration at the upper plane in the engine cylinder with the straight port.

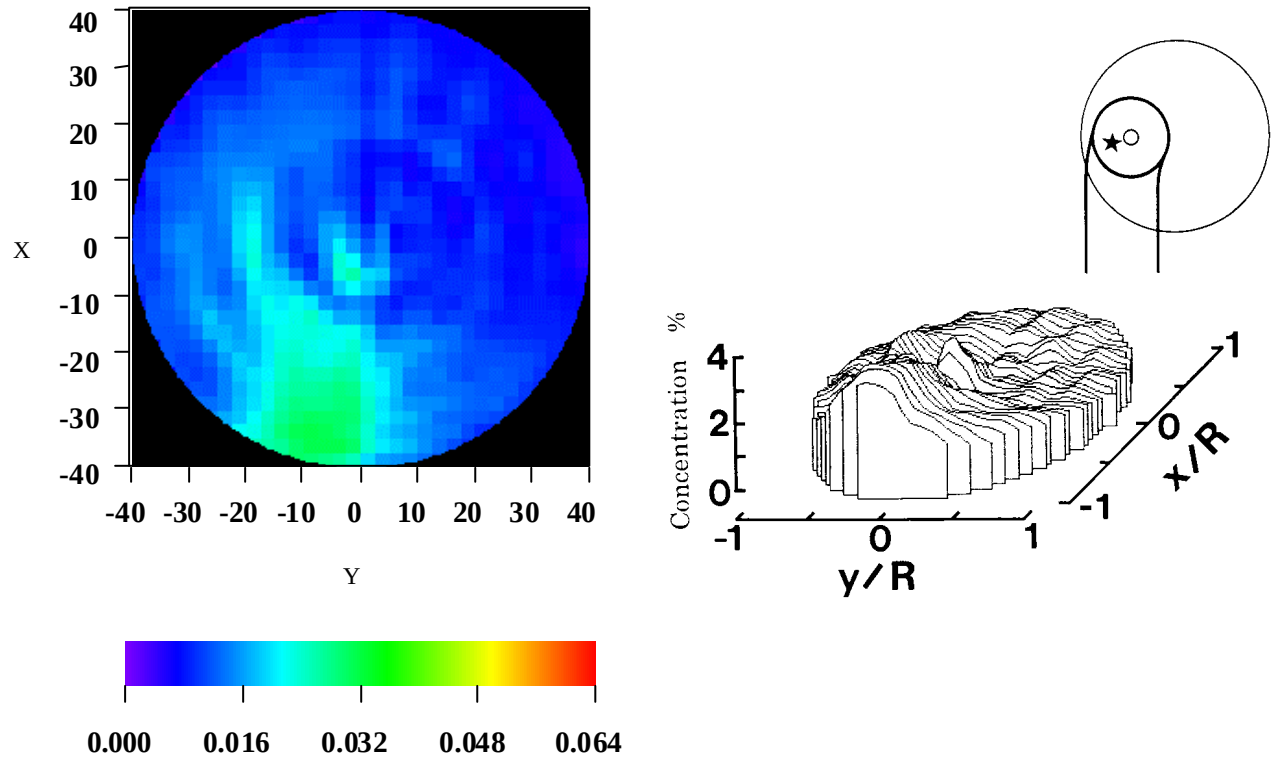

Fig.16 Methane concentration at the lower plane in the engine cylinder with the straight port.

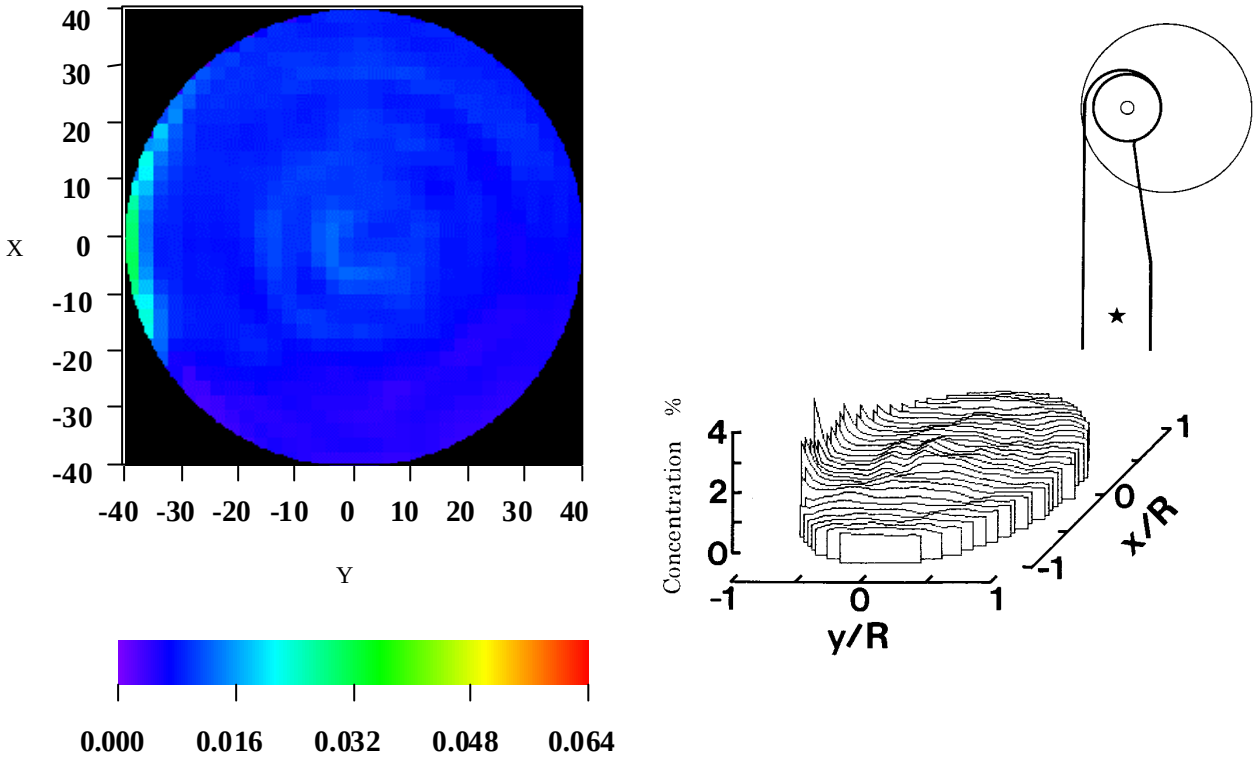

Fig.17 Methane concentration at the upper plane in the engine cylinder with the fuel injection upstream of the swirl port.

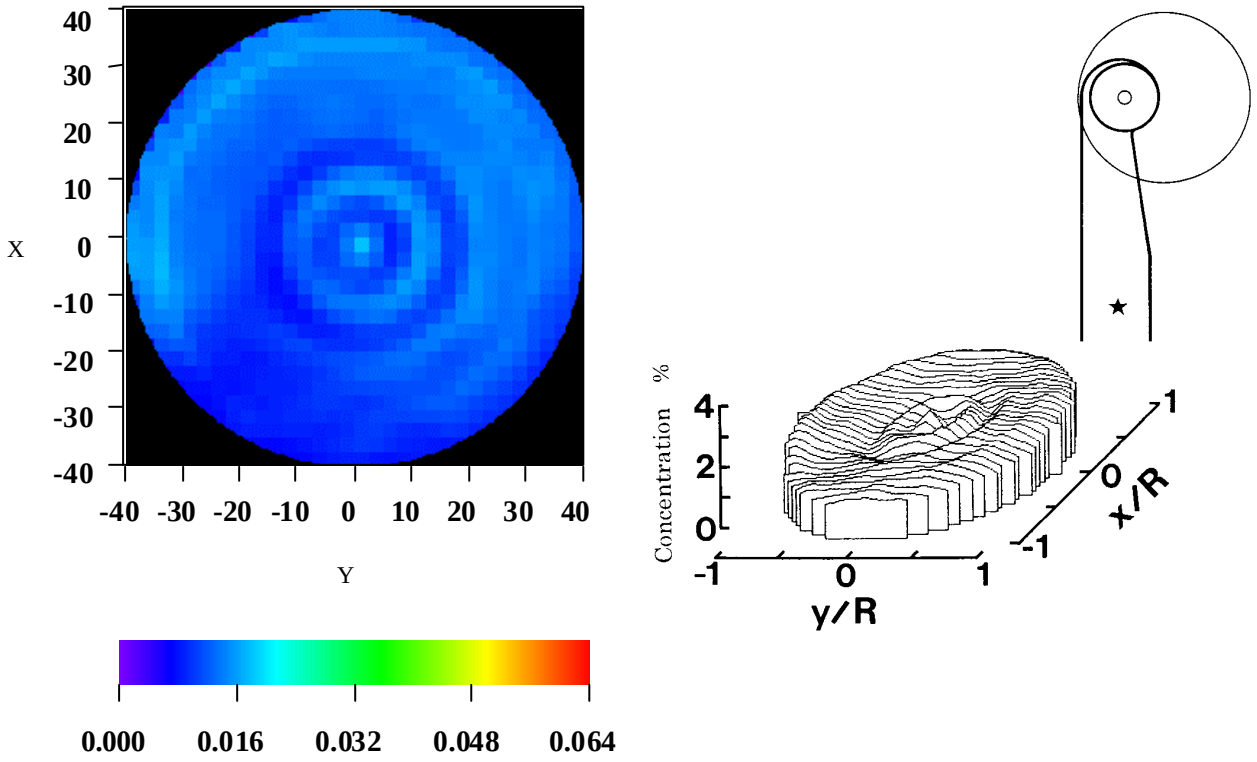

Fig.18 Methane concentration at the lower plane in the engine cylinder with the fuel injection upstream of the swirl port.

At the lower section, in figure 14, the location of the peak fuel concentration is shifted forward in the clockwise direction owing to the strong swirling flow and the peak decreases about one third of the result for z=10mm, 3.6%. Relatively rich fuel spreads forward from here by the convection effect of the swirl flow and the thin concentration extends from the back of the rich region to the opposite side of the region along the cylinder wall. Contrary to our expectations that diffusion of gaseous fuel would be promoted due to the both convection by swirling flow and diffusion by turbulence, an uneven distribution of the gaseous fuel is prolonged even at the lower section.

These results agree to the LDA measurement of the in-cylinder flow, that is, the air containing fuel just close to the cylinder wall below the intake valve goes downward and the air on the inner side flows clockwise horizontally by strong swirling motion. On the whole, qualitative gaseous fuel concentration could be verified spatially by the computer tomography method.

The results for the straight port case are shown in figures 15 and 16, corresponding to z=10 and 70mm. The peak of the fuel concentration becomes 4.9% and its location moves in the counter clockwise direction on the contrary to the result of the swirl port, while the global swirling motion in the cylinder is in the clockwise direction. Furthermore, the fuel convection/diffusion can be recognized toward the cylinder center, especially in lower plane. The fuel concentration peak is little rotated in the counter clockwise at the lower cross section of the cylinder and the peak decreases to be 3.2%. The inner-side wall of the intake ports caused the differences in the fuel to be directed towards the valve stem in the swirl port and generated strong swirl in the cylinder. On the whole, convection is superior to diffusion for spreading of gaseous fuel in engine cylinder, and therefore, fuel hardly spreads toward cylinder center for an engine with horizontal strong swirling flow like the swirl port results in the research.

Figures 17 and 18 show the results for the engine with the swirl port and fuel injection of 100 mm upstream of the intake valve. Although the upstream fuel injection results in homogeneous fuel concentrations at the lower plane, relatively rich concentration of fuel appears at the same location as that of the valve injection, where the fuel concentration has the peak of 3.1% which is one third of the valve fuel-injection result.

CONCLUSIONS

A new measuring method using computer tomography has been devised to analyze gaseous fuel distribution in an internal combustion engine. This technique is based on infra-red light absorption by C-H stretching vibration of hydrocarbon fuel molecules. The developed system was applied to in-cylinder flow in a gasoline engine model, and computed tomography measurement of the engine flow was successfully carried out by infra-red light fiber. It is found that while methane fuel was injected at the same location in engines with two types of intake ports, the fuel distributions were different with more fuel in the narrow area below the intake valve close to the cylinder wall at the upper cross section of the cylinder (z=10mm) in the case of the swirl port, and the half of the maximum fuel concentration in a wider and different region in the cylinder with the weaker swirl for the straight port case. The rich regions with the swirl port spread in the clockwise direction with the swirling flow at the lower plane (z=70 mm) and, with the straight port, moved counter-clockwise against the global direction of the weak swirling flow. It is apparent from all the results that the fuel did not diffuse quickly into the air and was convected so that the mixture was far from homogeneous even in the 70 mm plane. It is, of course, more homogeneous with upstream injection and also with the lower swirl number.

REFERENCES

[1] H. Kamura and K. Takada, Development of in-cylinder gasoline direct injection engine, JSAE Review, Vol.19, No.2, pp.175-180, 1998.

[2] M. Koike, A. Saito, D. Sawada and Y. Ishikawa, A New Concept of Direct Injection SI Gasoline Engine – Part1: Mixture Preparation Method -, Proc. JSAE, No.69-99 (in Japanese), 1999.

[3] M. Maeda, N. Sanai, K. Kobashi and K. Hishida, Measurement of Spray Mist Flow by a Compact Fiber LDV and Doppler-Shift Detector with a Fast DSP, Applications of Laser Anemometry to Fluid Mechanics, edited by R.J. Adrian et al., Springer-Verlag, pp.224-239, 1989.

[4] H. Kawazoe, K. Ohsawa and M. Kataoka, LDA Measurement of Gasoline Droplet Velocities and Sizes at Intake-Valve Annular Passage in Steady Flow State, Applications of Laser Anemometry to Fluid Mechanics, edited by R.J. Adrian et al., Springer-Verlag, pp.248-267, 1991.

[5] G. Wigley, G.K. Hargrave and J. Heath, High power, high resolution LDA/PDA system applied to gasoline direct injection sprays, Particle and Particle Systems Characterization, Vol.16, No.1, pp.11-19, 1999.
[6] M. Nagaoka, H. Kawazoe and N. Nomura, Modeling Fuel Spray Impingement on a Hot Wall for Gasoline Engines, SAE Paper, No.940525, pp.1-19, 1994.
[7] M. Posylkin, A.M.K.P. Taylor and J.H. Whitelaw, Manifold Injection and The Origin of Droplets at The Exit of An Inlet Valve, Proc. 7th Int. Symp Appl. Laser Tech. To Fluid Mech., Vol.2, pp.33.3.1-33.3.8, 1994.
[8] M.E.A. Bardsley, P.G.Felton and F.V. Bracco, 2-D Visualization of Liquid and Vapor Fuel in an I.C. Engine, SAE Paper, No.880521, pp.1-11, 1988.
[9] L.A. Melton and J.F Verdieck, Vapor/Liquid Visualization for Fuel Sprays, Combustion Science and Technology, Vol.42, p.217, 1985.
[10] R. Shimizu, S. Matsumoto, S. Furuno, M. Murayama and S. Kojima, Measurement of Air-Fuel Mixture Distribution in a Gasoline Engine Using LIEF Technique, SAE Paper, No.922356, pp.1-7, 1992.
[11] C. Arcoumanis et al,. SAE Paper, No.840376, 1987.
[12] I. Ebrahimi et al., Proceedings of International Symposium on Combustion, p.1711, 1976.
[13] K. Wakai, S. Shimizu and M. Kondo, Measurement of Two-Dimensional Temperature and Density Distributions by a 2-Band-Absorption CT, Trans. JSME, B, Vol.56, No.532, pp.346-351 (in Japanese) , 1990.
[14] B.C. Cuzzillo, J.T. Metcalf and J.W. Daily, Laser Absorption Measurement of Hydrocarbons in a Spark Ignition Square Piston I.C. Engine, Wss/CI Paper, No.82-59, pp.1-17, 1982.
[15] T. Tsuboi, K. Inomata, Y. Tsunoda, A. Isobe and K. Nagaya, Light Absorption by Hydrocarbon Molecules at 3.392 micro-meter of He-Ne Laser, Japanese Journal of Applied Physics, Vol.24, No.1, pp.8-13, 1985.
[16] Y. Ito, M. Kitaura and H. Fujimoto, Gaseous Fuel Concentration in Pre-chamber of Diesel Engine, Proc. of JSAE Conf., No.872, pp.637-642 (in Japanese), 1987.
[17] E Winklhofer, G K Fraidl and A Plimon, Monitoring of gasoline fuel distribution in a research engine, Proc Instn Mech Engrs, 206, pp.107-115, 1992.
[18] P.R. Shore and R.S. deVries, On-Line Hydrocarbon Speciation Using FTIR and CI-MS, SAE Trans., No.922246, pp.33-49, 1992.
[19] E.W. Rothe, Y. Gu, A. Chryssostomou, P. Andresen and F. Bormann, Effect of laser intensity and of lower-state rotational energy transfer upon temperature measurements made with laser-induced predissociative fluorescence, Applied Physics B: Lasers and Optics, Vol.66, No.2, pp.251-258, 1998.
[20] G. Herzberg, The Spectra and Structures of Simple Free Radicals, An Introduction to Molecular Spectroscopy, Cornell University Press, New York, 1971.
[21] J. Radon, Uber die Bestimmug von Funktionen durch Ihre Integralwerte Laengs Geweisser Mannigfaltigkeiten, Berichte Saechsishe Acad. Wissenschaft. Math. Phys., Klass 69, pp.262-271, 1917.
[22] R. Gordon and G.T. Herman, Three dimensional reconstruction from projection – A review of algorithms-, Int. Rev. Cytol., Vol.38, pp.111-151, 1974.
[23] R. Gordon, et al., Algebraic reconstruction technique (ART) for three dimensional electron microscopy and X-ray photograph, Jour. Theor. Biol., Vol.29, pp.471-481, 1970.
[24] D.B. Kay, et al., Jour. Nucl. Med., Vol.15, p.981, 1974.
[25] T.F. Budinger and G.T. Gullberg, IEEE Trans. Nucl. Sci., Vol..NS-21, p.2, 1974.
[26] L.A. Shepp and B.F. Logan, The Fourier reconstruction of a head section, IEEE Trans. Nucl. Sci., Vol.NS-21, pp.21-43, 1974.
[27] M. Nakayama and T. Araki, A Study of Visualization of Diesel Spray by Means of Computed Tomography, Trans. JSME, B, Vol.54, No.501, pp.1193-1188 (in Japanese), 1988.